JOURNAL OF APPLIED PHYSICS **97**, 114904 (2005)

Effect of ozone treatment on the electrical properties of $(Ba_{0.7}Sr_{0.3})TiO_3$ thin films

Sandip Halder[a] and Theodor Schneller
Institute for Materials in Electrical Engineering and Information Technology-II [Institut für Werkstoffe der Elektrotechnik II (IWE-II)] Rheinische Westfäliche Technische Hochschule (RWTH) Aachen, D-52056, Aachen, Germany

Rene Meyer and Rainer Waser
Institut für Festkoerperforschung (IFF), Forschungszentrum Juelich, D-52425, Juelich, Germany

(Received 20 December 2004; accepted 5 April 2005; published online 25 May 2005)

Thin films of $(Ba_xSr_{1-x})TiO_3$ were deposited on Pt-coated Si substrates by chemical solution deposition. The films were postannealed under ozone atmosphere at various temperatures. Although there was no change observed in the microstructure after the anneal in ozone, the dielectric dispersion and the loss tangents were reduced for the films. It was also noticed that the leakage current reduced by almost two orders of magnitude after treatment with ozone. The ozone treatment was done at various temperatures between 250 and 450 °C to find an optimum temperature with regard to the electrical properties. Films postannealed in ozone at 350 °C for 30 min showed a leakage reduction by almost three orders of magnitude. The leakage dependence on ozone postannealing is discussed on the basis of an interface-dominated (Schottky injection) and a bulk-dominated (point defect approach) charge transport process as the two limiting conduction mechanisms across thin films. © *2005 American Institute of Physics*. [DOI: 10.1063/1.1927289]

I. INTRODUCTION

Perovskite thin films have been intensely investigated as a high permittivity dielectric for a variety of integrated devices. One potentially suitable material for these applications is $(Ba_xSr_{1-x})TiO_3$ (BST).[1] The substitution of Ba with Sr leads to the shifting of the Curie point to lower temperatures. The cubic-paraelectric phase of BST displays less dielectric loss in comparison with pure BT and there is no ferroelectric hysteresis in the capacitance–voltage sweeps. These characteristics enable BST to be used for such varied applications as phase shifters,[2] decoupling capacitors, and tunable microwave devices.[3] For most cases a high tunability and low loss tangents are required.[4] The particular composition with $x=0.7$ is one of the most extensively researched BST systems.

Thin films of BST have been deposited by a variety of methods such as metal-organic chemical-vapor deposition (MOCVD), sputtering,[5] pulsed laser deposition (PLD),[6] and chemical solution deposition (CSD).[7] At present CSD is one of the most commonly used methods for deposition of thin films because of its ease and its high stoichiometric control in the final processed films.

Processing of BST films remains an important issue in view of such varied applications. In most electrical devices leakage properties are an important factor. The lesser the leakage the better the device performance. Therefore any such development, which reduces leakage in such thin films, is of great importance.

II. EXPERIMENT

BST thin films were made by chemical solution deposition of a 0.1-M propionic acid-based precursor solution on Pt-coated Si substrates. Details of the solution preparation have been provided elsewhere.[8,9] After the deposition each layer is crystallized at 700 °C for 10 min, which had been optimized for maximum crystallinity and duration. This process is repeated 22 times until the films reach a thickness of approximately 200 nm. Pt is sputter deposited on these films and then structured into 0.07-mm^2 top electrodes by a photolithographic lift-off process.

The electrical properties of differently postannealed crystalline films will be discussed. Unannealed films strictly refer to films without any type of postannealing after top electrode deposition. All the other films after electrode deposition have been annealed in oxygen for 5 min at 700 °C in a rapid thermal annealing (RTA) unit. For the ozone annealed films, after the top electrode is annealed in oxygen in RTA for 5 min, it is annealed again in ozone for 30 min at different temperatures. This sequence is important because it was noticed that if the films were annealed in the RTA with oxygen after the ozone anneal then the leakage of the films again increased. The RTA step could not be excluded because it ensures a good contact between the top electrode and surface. The ozone annealing was performed at different temperatures (250, 300, 350, and 400 °C) to investigate the effect on the leakage current. An Ozomatic (Modular HC-Series) ozone generator was used for generating the ozone. The ozone concentration was maintained at 4 gm/h for all the ozone annealing processes.

III. RESULTS AND DISCUSSION

From the scanning electron microscope pictures it can be clearly seen that the films have a columnar structure, as shown in Fig. 1. The columnar structure of the films is, in fact, responsible for its higher dielectric constant. Films,

[a]Electronic mail: halder@iwe.rwth-aachen.de

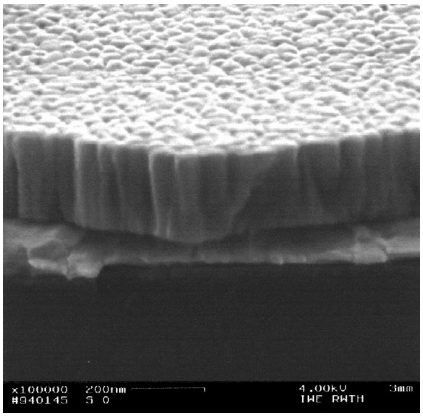

FIG. 1. Scanning electron microscopy (SEM) picture of the films deposited on Pt wafers showing a columnar structure.

which are deposited from solutions with a concentration higher than 0.15 M, yield films with smaller grains and lower dielectric constant.[10] Since the x-ray diffraction patterns show no increase in crystallinity after postannealing in ozone it is not shown here. Furthermore, the ozone annealing has no influence on the microstructure or the crystallization temperature. This was proven in a separate set of experiments where amorphous films were deposited layer by layer at room temperature and then crystallized directly in an ozone atmosphere at various temperatures between 300 and 700 °C. These films, which were annealed at temperatures below 600 °C, show no sign of any crystallization when checked by glancing angle x-ray diffraction (not shown here). For films above 600 °C usually there is some degree of crystallization but this is true even for films when annealed in pure oxygen. Hence it is impossible to say whether the effect is from ozone or from oxygen. Furthermore at such high temperatures the existence of molecular ozone is questionable.[11] Hence these films will not be discussed further. We will concentrate only on the ozone postannealing effect of fully crystalline films.

The dielectric constant versus frequency is measured for the different films. It was noticed that after the films were postannealed in oxygen and ozone the dissipation factor decreased. The films which were unannealed showed larger dispersion, as evident from Figs. 2(a) and 2(b). The dielectric constant versus voltage of the different films is shown in Fig. 3. In our case, the slightly higher average dielectric constant of the nonpostannealed films can be explained on the basis of a change in the rough top interface. As the films are postannealed in oxygen for 5 min at 700 °C, prior to annealing in ozone again (between 250 and 400 °C), the rough top surface becomes smooth. That the top interface between the Pt and BST changes from a very rough to a smooth interface, on postannealing in oxygen, has recently been shown by our group.[12] In addition the field distribution in such rough-surfaced structure could also become nonhomogeneous leading to further complications. However, possibilities of changes in the interface capacitance, caused during the sputter deposition of top electrodes, cannot be ignored, since any change in them would manifest a change in the dielectric constant. Any one or a combination of the above can produce an effect on the dielectric constant.

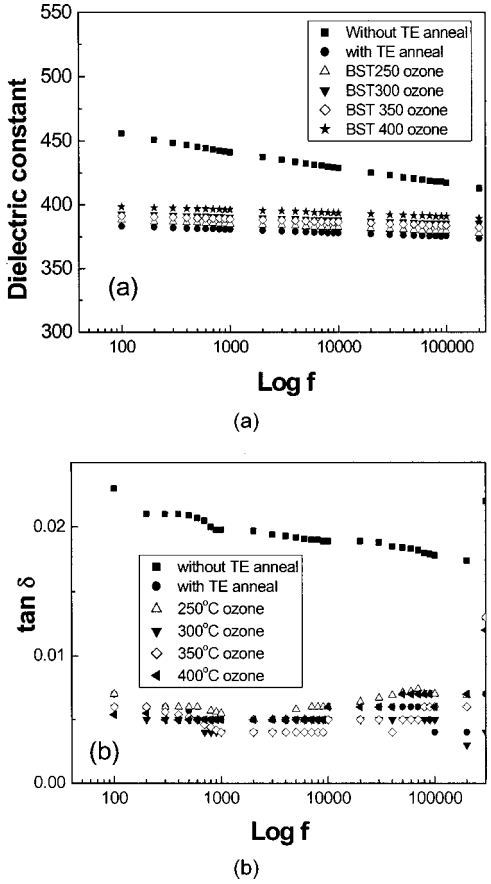

FIG. 2. (a) Dielectric constant vs frequency of the different films. Films annealed in ozone show a slight increase in the dielectric constant. (b) The loss tangents vs frequency of the different films. It was noticed that films which were postannealed in ozone showed a lowering of the loss tangents and its lowest for films postannealed in ozone at 350 °C.

The tunability $(\varepsilon_{max}-\varepsilon_{min}/\varepsilon_{max})$ of the films was found to be approximately between 38% and 42% for the oxygen and ozone annealed films. The tunability of the films is comparable to bilayer films deposited by rf sputtering recently reported by Xia *et al.*[13] The films which were not annealed in oxygen or ozone show a somewhat shifted curve and the reason for such a shift is the difference in the top and bottom electrode interfaces. The dissipation factor reduces once the films have been annealed in oxygen or ozone. However,

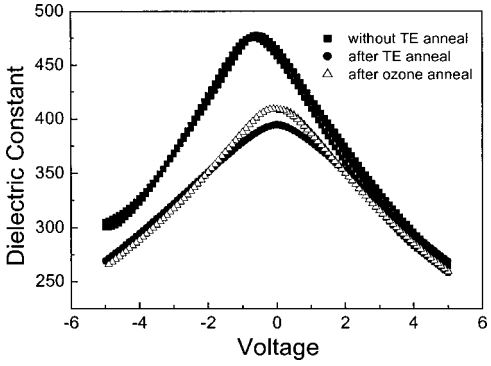

FIG. 3. Dielectric constant vs voltage for only the films postannealed in ozone at 350 °C is shown in comparison with films without top electrode annealing and films with top electrode annealing in oxygen. Note the slight shift in the curve for films without the top electrode anneal.

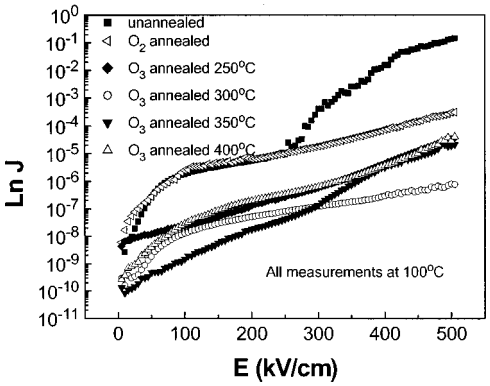

FIG. 4. Leakage measurements of the different films at 100 °C. The leakage is found to decrease after ozone postannealing until 350 °C, however, beyond that it increases again.

there is a slight increase of the dielectric constant with the increase of ozone annealing temperature. Beyond 400 °C the ozone annealing did not produce any further increase of the dielectric constant. The increase of the dielectric constant on ozone annealing could be due to the change in the interface capacitance.

An important property of perovskite-type titanate thin films is the charge transport mechanism. The dc leakage currents were evaluated using a step voltage technique. For the step voltage technique a voltage is applied to the sample and current flow is measured as a function of time, at times lesser than some crossover time this measurement is dominated by some polarization current, while at times longer than this it is dominated by the true leakage current.

Figure 4 shows the variation in leakage current density with applied electric field for the unannealed, oxygen annealed, and ozone annealed BST thin films. It is noticed that the leakage was reduced after an ozone anneal. The reduction in leakage was also dependent on the temperature of the ozone anneal. Films, which were annealed at 350 °C in ozone, showed the lowest leakage because of O atoms diffusing through the film, thereby reducing the number of oxygen vacancies. Any further increase in the ozone annealing temperature did not help in reducing the leakage any further. With increase of temperature the decomposition of ozone into O_2 and O radicals also increases and beyond a certain temperature the collision frequency of the radicals increases and instead of O radicals there is O_2 formation before the wafer is reached.

Two basic mechanisms, charge injection from the electrode (Schottky mechanism) as an interface limiting transport process and the reduction of oxygen vacancies inside the thin film via point defect reaction during equilibration in ozone as a bulk limiting transport process, are discussed.

A. Interface limiting charge transport mechanism (Schottky injection)

We commence with the standard reverse-biased Schottky equation. This equation is widely applied to the leakage current data analysis for perovskite-type titanate thin films[14,15] and it can be expressed as follows:[16]

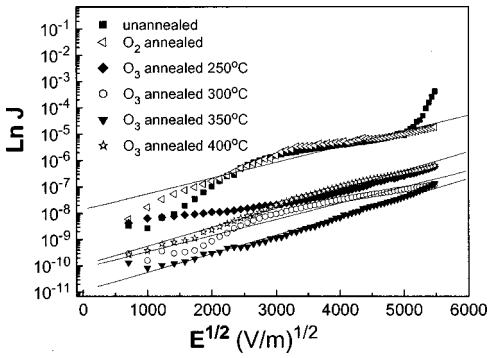

FIG. 5. $\ln J$ vs $E^{1/2}$ plots of the different films. The plots are linear for the ozone annealed films.

$$J = AT^2 \exp\left(\frac{\alpha E^{1/2} - W_b}{k_B T}\right), \quad \alpha = \left(\frac{q^3}{4\pi\varepsilon_r\varepsilon_a}\right)^{1/2}. \tag{1}$$

Agreement with the Schottky barrier model can be verified by plotting the values of $\ln J$ vs $E^{1/2}$ for moderately high electric fields.[17,18] From the above equation it automatically follows that such a plot should be linear for the Schottky mechanism to be dominant. The value of α is extracted from the slope of this plot and then taken with the slope of the $\ln J/T^2$ vs $1000/T$ plot to determine the barrier height.

Figure 5 shows the $\ln J$ vs $E^{1/2}$ plots. All the films show a linear region at moderately high fields. This is expected if the leakage current obeys the Schottky mechanism. Figure 6 shows the plot of the $\ln J/T^2$ vs $1000/T$ plot, which also is linear. The barrier heights for the different films are calculated and shown in Fig. 7. It is seen that the barrier heights increase until a postannealing temperature of 350 °C in ozone. This may explain why there is a reduction of leakage current under conditions that are dominated by the Pt/BST Schottky barrier.[19]

B. Bulk-limited charge transport mechanism (point defect approach)

Conductivity studies of BST ceramics and STO single crystals under various oxygen partial pressures have shown that the bulk conductivity of undoped and acceptor-doped STO and BTO is a function of the oxygen activity. A point defect model giving rise to the pO_2 dependence predicts a reduction of oxygen vacancies upon oxidation according to the point defect reaction

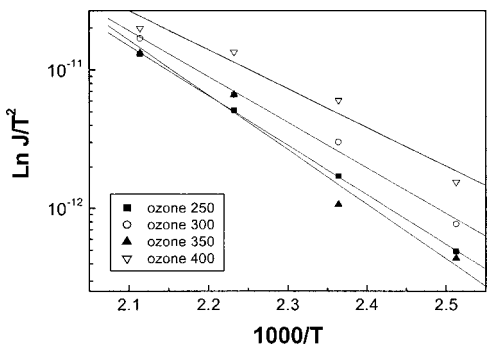

FIG. 6. $\ln J/T^2$ vs $1000/T$ plots of the different films from which the barrier heights were extracted.

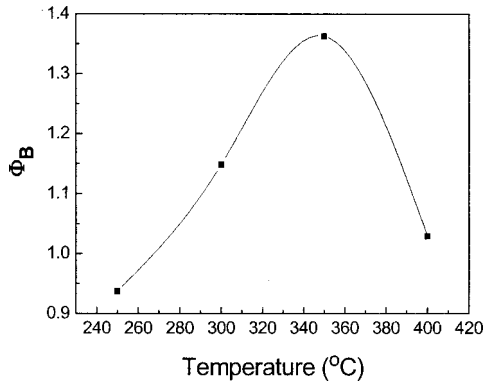

FIG. 7. A plot of the different barrier heights vs the ozone postannealing temperature. The barrier height is highest for the films postannealed in ozone at 350 °C which might be a cause for its low leakage current.

$$\frac{1}{2}O_2(g) + 2e' + V_O'' \underset{\text{red.}}{\overset{\text{ox.}}{\Leftrightarrow}} O_O^x. \tag{2}$$

Here, e' denotes the electrons, V_O'' is a vacancy on an oxygen lattice site, and O_O^x denotes oxygen on its regular crystallographic site (Kroger–Vink notation). Following Eq. (2), an increase in the oxygen activity is linked to declining electron conductivity, since electrons are consumed, when positively oxygen vacancies are filled with oxygen. In particular, the defect situation in thin films is more complicated. For example, the electron-hole equilibrium causes an increase of holes, if the concentration of electrons is reduced. Furthermore, a heterogeneous defect concentration across the film has to be assumed.

So far, the complex defect situation in thin films is only fairly understood and hence, still under investigation. We will therefore not go into more detail, but will only present some results of a model system to show the tendency.

Figure 8(a) displays the defect distribution of oxygen vacancies, electrons, and holes for a given temperature and oxygen partial pressure. The contact potential at the top and the bottom interface is assumed to be phi=1.2 eV, which may represent the contact potential at the Pt/BST interface. An acceptor impurity concentration was assumed to $Na=1\times18\ cm^{-3}$. First, we let the system equilibrate at 600 °C to simulate the postannealing step. After equilibration, the system was quenched to 200 °C the new electronic equilibrium was calculated. Oxygen exchange with the ambient was considered not to occur at low temperatures. We find the formation of a Schottky-type contact, thereby the space-charge layer near the interface is not formed by depletion in electronic charge carrier, but the repellence to ionic oxygen vacancies caused by a charge transfer of electrons from the electrode into the film.

Figure 8(b) illustrates the effect of a postanneal under higher oxygen partial pressure. Based on the defect reaction given in Eq. (2), the concentration of oxygen vacancies is reduced in the vicinity of the interface. Note that the concentration of electrons and holes at the interface is kept constant due to the constant contact potential. Here, the formation of *pn* junctions in the thin film is found. From the local concentrations of electronic charge carriers, the film resistance is estimated for small signal excitation. Figure 9 shows the film

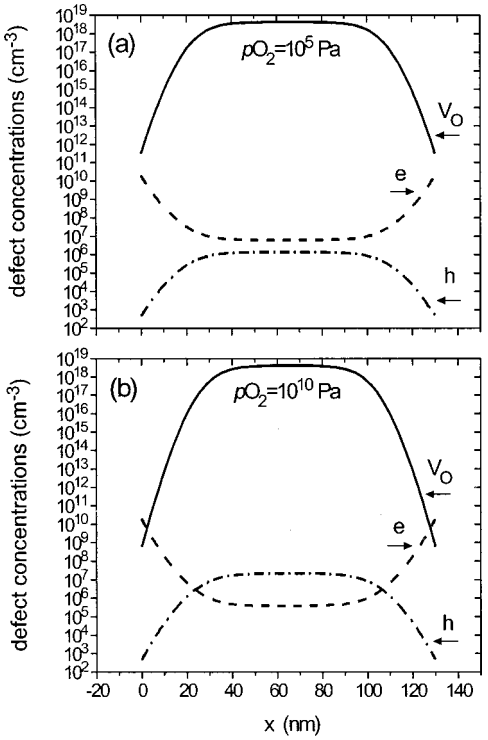

FIG. 8. Defect distribution of oxygen vacancies (V_O), electrons (e), and holes (h) of a Pt/BST/Pt structure at 200 °C equilibrated at 600 °C at (a) $pO_2=10^5$ Pa and (b) $pO_2=10^{10}$ Pa. The formation of *pn* junctions reduces the conductivity of the film exposed to the higher oxygen activity.

resistance for postannealing under 1 Pa (N_2), 10^5 Pa (O_2), and 10^{10} Pa (assumed for the oxygen activity in the case of ozone treatment).

At this point, it should be mentioned that the presented calculations can just be regarded as a first-order approximation to demonstrate the influence of ozone postanneal in general. Various parameters such as the impurity acceptor concentration, the cation vacancy concentration, a special distribution of defects, trapping effects at the interface and in the thin-film itself, a lowering of the contact potential by image forces, low-k interfacial layer, and a large signal band bending have not yet been considered.

Whether the charge transport is interface limited or bulk limited may also depend on exposing the thin film to moderate or large voltages. Since both mechanisms predict a re-

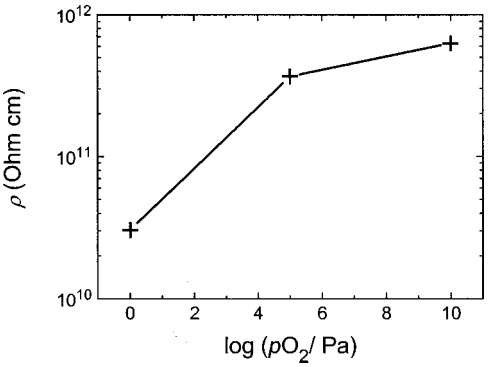

FIG. 9. Calculated small signal resistivity of a 130-nm-thick BST thin film at 200 °C as a function of the postannealing under different oxygen partial pressures at 600 °C.

duction of the leakage current, further investigation is needed to elucidate the dominating charge transport mechanism.

IV. CONCLUSIONS

Thin films of BST were deposited by CSD on Pt-coated Si substrates. These films were then treated with ozone after a top electrode anneal at various temperatures between 250 and 400 °C. On ozone annealing the dielectric constant of the films was found to increase. The leakage current was found to decrease by almost three orders of magnitude after an ozone anneal at 350 °C. The results were discussed on the basis of the Schottky injection model describing an interface-limited charge transport and the removal of oxygen vacancies followed from a point defect approach, which comes into play, if the charge transport is dominated by the bulk rather than the interface.

[1]D. E. Kotecki, J. D. Baniecki, H. Shen, and S. D. Athavale, IBM J. Res. Dev. **43**, 367 (1999).
[2]Y. Liu, A. S. Nagra, E. G. Erker, P. Periaswamy, T. R. Taylor, J. S. Speck, and R. A. York, IEEE Microw. Guid. Wave Lett. **10**, 448 (2000).
[3]B. A. Baumert, L.-H. Chang, A. T. Matsuda, C. J. Tracy, N. G. Cave, R. B. Gregory, and P. L. Fejes, J. Mater. Res. **13**, 197 (1998).
[4]Q. X. Jia, J. R. Groves, P. Arendt, A. T. Findikoglu, S. R. Foltyn, H. Jiang, and F. A. Miranda, Appl. Phys. Lett. **74**, 1564 (1999).
[5]Y. Xia, D. Wu, and Z. Liu, J. Phys. D **37**, 2256 (2004).
[6]S. Saha and S. B. Krupanidhi, J. Appl. Phys. **87**, 849 (2000).
[7]R. W. Schwartz, T. Schneller, and R. Waser, C.R. Acad. Sci., Ser. IIc: Chim **7**, 433 (2004).
[8]U. Hasenkox, S. Hoffmann, and R. Waser, J. Sol-Gel Sci. Technol. **12**, 67 (1998).
[9]S. Hoffmann and R. Waser, J. Eur. Ceram. Soc. **19**, 1339 (1999).
[10]C. L. Jia, K. Urban, S. Hoffmann, and R. Waser, J. Mater. Res. **13**, 2206 (1998).
[11]C. Isobe and M. Saitoh, Appl. Phys. Lett. **56**, 907 (1990).
[12]Y. L. Qin, C. L. Jia, K. Urban, R. Liedtke, and R. Waser, Appl. Phys. Lett. **80**, 2728 (2002).
[13]Y. Xia, D. Wu, and Z. Liu, J. Phys. D **37**, 2256 (2004).
[14]J. F. Scott and M. Azuma, Proceedings of the ISAF, 1992 (unpublished), p. 356.
[15]S. T. Chang and J. Y. Lee, Appl. Phys. Lett. **80**, 655 (2002).
[16]S. M. Sze, *Physics of Semiconductor Devices*, 2nd ed. (Wiley, New York, 1981).
[17]G. W. Dietz, M. Schumacher, R. Waser, S. K. Streiffer, C. Basceri, and A. I. Kingon, J. Appl. Phys. **82**, 2359 (1997).
[18]C. S. Hwang *et al.*, J. Appl. Phys. **83**, 3703 (1998).
[19]M. Copel, J. D. Baniecki, P. R. Duncombe, D. Kotecki, R. Laibowitz, D. A. Neumayer, and T. M. Shaw, Appl. Phys. Lett. **73**, 1832 (1998).